Spatial and Temporal Change Monitoring of Wetland Urban Ecology Based on a Remote Sensing Ecological Index Considering Full Elements

Jiao Pan, Ziwei Wang, Tao Chen, *Senior Member, IEEE*, Kun Jia, and Antonio Plaza, *Fellow, IEEE*

***Abstract*—Influenced by the exploitation of natural resources and industrialization, ecological and environmental problems have become increasingly severe worldwide, particularly in rapidly developing countries such as China. This study utilizes Earth observation satellite data to monitor changes in ecological environment quality of the Wuhan Urban Development Zone (WUDZ) from 2000 to 2020, employing the remote sensing ecological index considering full elements. By incorporating water bodies into the calculation through the entropy weight method and moving window, this approach takes into account the benefits of water elements on the overall ecological environment (EE). The results indicate the following: 1) from 2000 to 2020, the overall EE of WUDZ exhibited an initial improvement followed by a subsequent decline, with minor fluctuations. 2) The EE of WUDZ is dominated by greenness and dryness. The central and main urban areas have poorer ecological environment quality compared to the urban development area, while remote suburban areas experience gradual deterioration as progression of urbanization. 3) The primary driving factors for ecological environment quality changes in WUDZ are increased urbanization and lake resource erosion. This study provides a quantitative method for the temporal monitoring of wetland urban EE, and provides a scientific basis for the rational formulation of policies and planning for the development of lake ecological space and the restriction of urban construction space.**

Manuscript received 4 March 2024; revised 25 June 2024; accepted 22 July 2024. Date of publication 30 July 2024; date of current version 15 August 2024. This work was supported in part by the National Natural Science Foundation of China under Grant 62371430, and Grant 62071439, in part by the Open Fund of State Key Laboratory of Remote Sensing Science under Grant OFSLRSS-202207, in part by the Opening fund of State Key Laboratory of Geohazard Prevention and Geoenvironment Protection (Chengdu University of Technology), under Grant SKLGP2022K016, in part by the Open Fund of Badong National Observation and Research Station of Geohazards under Grant BNORSG-202302, and in part by Opening Fund of the Key Laboratory of National Geographic Census and Monitoring, Ministry of Natural Resources, under Grant 2023NGCM11. *(Corresponding author: Tao Chen.)*

Jiao Pan and Ziwei Wang are with the Institute of Geophysics and Geomatics, China University of Geosciences, Wuhan 430074, China (e-mail: pan@cug.edu.cn; wzw2020@cug.edu.cn).

Tao Chen is with the School of Geophysics and Geomatics, China University of Geosciences, Wuhan 430074, China, also with the State Key Laboratory of Remote Sensing Science, Faculty of Geographical Science, Beijing Normal University, Beijing 100875, China, also with the Badong National Observation and Research Station of Geohazards, China University of Geosciences, Wuhan 430074, China, and also with the Key Laboratory of National Geographic Census and Monitoring, Ministry of Natural Resources, Wuhan 430079, China (e-mail: taochen@cug.edu.cn).

Kun Jia is with the Institute of Beijing Engineering Research Center for Global Land Remote Sensing Products, Faculty of Geographical Science, Beijing Normal University, Beijing 100875, China.

Antonio Plaza is with the Hyperspectral Computing Laboratory, Department of Technology of Computers and Communications, Escuela Politecnica, University of Extremadura, 10071 Caceres, Spain (e-mail: aplaza@unex.es).

Digital Object Identifier 10.1109/JSTARS.2024.3435559

***Index Terms*—Ecological benefits of water bodies, ecological environment (EE), remote sensing ecological index, spatial and temporal change monitoring, wetland urban.**

I. Introduction

PRESENTLY, China stands out as the developing country experiencing the most rapid urbanization. The relentless expansion of cities and swift economic growth have exerted a profound impact on urban ecological spaces [1]. Consequently, the ecological environment (EE) has undergone severe deterioration, giving rise to a spectrum of issues including air pollution [2], vegetation destruction [3], urban heat islands [4], land occupation [5], and urban flooding [6]. Human survival and development hinge on a suitable environment, yet our economic and social progress has inflicted damage on the environment, posing a threat to sustainable development [7]. Amidst the imperative of ensuring rapid and high-quality urban development, the focal point has shifted toward protection of regional EE. Achieving coordination between urban development and the environment emerges as a pivotal challenge in urban construction [8]. Therefore, conducting comprehensive, efficient, and accurate monitoring and evaluation of the urban EE, coupled with an analysis of its integration with urban construction activities and spatial changes in the city's natural resources, holds paramount significance. Such an approach is crucial for formulating policies that safeguard EE and promoting the sustainable development of cities.

With the advancement of Earth observation technology and digital image processing, it has become possible to swiftly identify spatial and temporal changes in the EE. These technologies provide a convenient means to assess EE accurately and rapidly, thereby revolutionizing traditional evaluation methods [9], [10], [11]. The quality of the EE encompasses various ecological indexes. Previous studies on remote sensing-based monitoring of EE time series have often relied on single indicators model [12], such as the normalized difference vegetation index (NDVI) [13], enhanced vegetation index [14], and land surface temperature (LST) [15]. However, given the complexity inherent in ecosystems, a single indicator may not comprehensively reflect the status of regional EE. In response to this limitation, scholars have proposed comprehensive evaluation index systems. Among these, widely utilized models include the environmental quality index [16], ecological index [17], pressure-state-response model

[18], and the remotely sensed ecological index model (RSEI) [19]. The RSEI model has been widely applied to study changes in regional EE time series in mining areas [20], cities [21], and watersheds [22]. Its advantages lie in being entirely based on remotely sensed imagery and having access to historical archival data.

In recent years, increased understanding of ecological impact mechanisms and the increasing deployment of high-resolution sensors on Earth observation satellites have greatly enriched the available research data, some scholars have proposed to use targeted index models to evaluate the temporal changes of EE under special ecological background. Examples of these approaches include arid remote sensing ecological index [23] for evaluating ecological conditions in desert areas, the moving window-based RSEI [24] for ecological monitoring in mining areas, and the RSEI based on granular entropy knowledge [25]. However, the utilization of RSEI still encounters certain limitations [26]. First, in extreme EE such as deserts, the application of the model is limited, leading to unstable results [15], [27]. Second, the contribution rate of the first principal component typically falls between 60% and 90%, lacking a fixed standard. Relying solely on the plus or minus sign of the contribution value in principal component analysis to illustrate the impact of index on the EE is inaccurate and may result in the loss of detailed information [28]. Third, the expression of ecological element information is incomplete. The model calculation excludes water element information due to the characteristics of principle component analysis method, thereby neglecting the ecological benefits produced by water bodies in the regional ecological assessment. Since ecological environment quality (EEQ) reflects the feedback effect of a comprehensive set of elements in space, the lack of certain elements can lead to an inaccurate expression of the surface EE [29].

In order to overcome the above shortcomings, this article selects the remote sensing ecological index considering full elements (RSEIFE) [30], which incorporates water bodies into the RSEI calculation process through the entropy weight method and moving window (ecological impact range window). This model fully considers the ecological elements of the ground features and the relationship between adjacent ground features. This approach allows for a more stable E assessment in both space and time. The wetland city (Wuhan City) was selected as the study area, and the regional EE time series was monitored and evaluated.

The main contributions of this work are as follows.

1) Savitzky–Golay (SG) filtering is used to reconstruct the time series, retaining the linear trend of the original data while removing irregular fluctuations.
2) RSEIFE can fully consider the characteristics of water bodies and their ecological benefits to the regional environment.
3) EEQ in the study area generally increases first and then decreases, with changes in urban EE driven by both natural resource transfer and human activities.

The rest of this article is organized as follows. Section II describes the data used in the work. Section III introduces the methods used in this article. Section IV gives the results. The discussion is given in Section V. Finally, Section VI concludes this article.

II. Study Area and Data

A. Study Area

The study area is located at Wuhan Urban Development Zone (WUDZ) in the middle reaches of the Yangtze River (29°58′–31°22′N, 113°41′–115°05′E) with an area of 3261.16 km^2 (see Fig. 1). This region is characterized by a subtropical monsoon climate, featuring abundant rainfall, a mild climate, and four distinct seasons. The average annual temperature ranges from 15.8 to 17.5 °C, while the average annual rainfall ranges between 1150 and 1450 mm.

The research area is known as an international wetland city, with an extensive river network and dense lakes, and the city's wetland area is 1624.61 square kilometers, accounting for 18.9% of the total area. The abundant wetland resources play an important role in regulating the regional EE. However, the phenomenon of "enclosing lakes to make fields" and urban expansion has resulted in the substantial filling and occupation of lakes. This has led to a reduction in the number and area of lakes, an increase in water pollution, and a degradation of the EE. These changes and damages have adversely affected the storage function of lakes, subsequently impacting the climate of the surrounding areas. Consequently, various ecological and environmental problems have arisen.

B. Data and Preprocessing

The data used in this study include lake vector range, administrative boundary[1] and annual China land cover dataset. Among them, the dataset includes Earth observation satellite data from Landsat 5 TM, Landsat 7 ETM+, and Landsat 8 OLI/TIRS SR Surface Reflectance Database, as well as DEM data (NASA SRTM digital elevation at 30 m spatial resolution). To account for changes in plant phenological transition periods, images from June to September were specifically selected for subsequent experiments using a temporal filter function. The remote sensing data, accessed through the GEE (Google Earth Engine) platform, consist of surface reflectance data that have undergone radiometric calibration and atmospheric correction. These data are further processed through regional filtering, declouding, and median synthesis. For constructing the surface temperature index, thermal infrared bands are resampled to a 30 m spatial resolution.

The land use and land cover data used in this article come from the CLCD2021 national land cover data (30 m spatial resolution) [31]. The dataset includes nine main land cover types: cropland, forest, shrub, grassland, water, ice and snow, bare land, construction land, and wetlands. For this experiment, the land use and land cover data of the years 2000, 2005, 2010, 2015, and 2020 were downloaded and tailored according to the study area.

[1]Online. [Available]: http://gtghj.wuhan.gov.cn/pc-69-35849.html

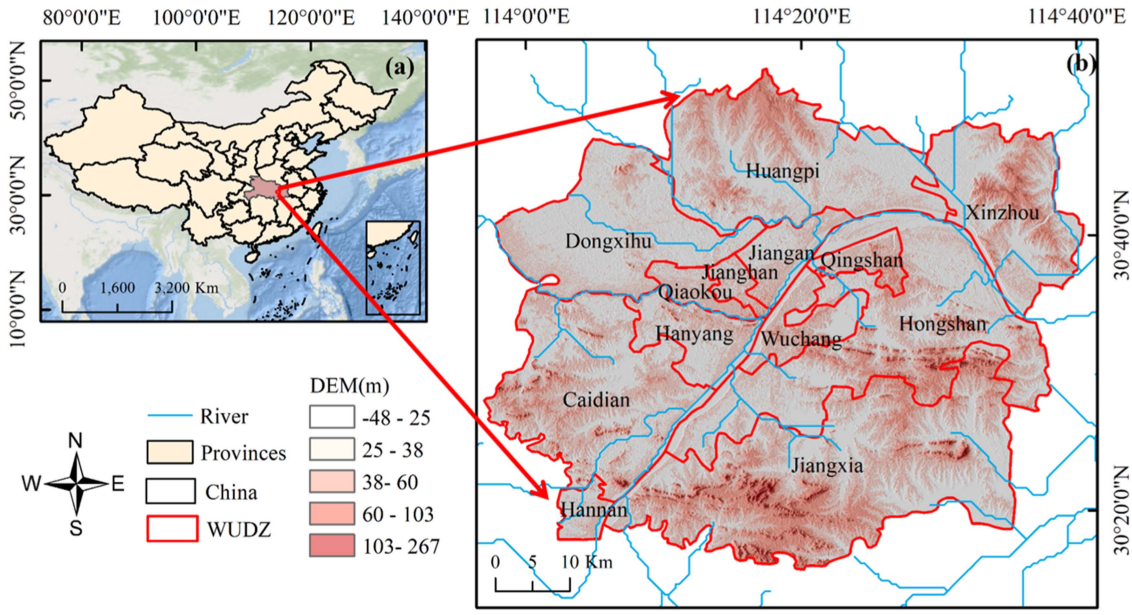

Fig. 1. Location of the study area.

III. Methodology

A. Savitzky-Golay Filtering Method

The SG filtering method is a local filtering algorithm based on the principle of least squares [32], the algorithm uses high-order polynomials to carry out the least squares fitting in the sliding window. The algorithm uses high-order polynomials for least squares fitting within a sliding window, if the time-series variation of indexes adheres to basic seasonal and inter-annual characteristics. It further presupposes that the most of noise in the data should be lower than the average of the time-series data, which has been widely utilized in reconstructing time-series data such as vegetation index, leaf area index, surface wetness, surface temperature, and RSEI. Therefore, in this study, the SG filtering method was chosen to reconstruct the ecological index with the following formula:

$$Y_j^* = \frac{\sum_{i=-m}^{i=m} C_i Y_{j+i}}{N} \tag{1}$$

where Y_{j+i} is the original value of the index; Y_j^* is the smoothed value of the index; C_i is the weight index of the ith index value in the smoothing window, j is the original index array coefficients; m is the half-width of the smoothing window; and N denotes the size of the smoothing window.

B. Remote Sensing Ecological Index

RSEI [33] model refers to the four ecological indexes of greenness, wetness, dryness, heat to represent the state of regional EEQ. The four ecological indexes were represented by the NDVI [34], the moisture component of cap changes [35], [36], dryness index synthesized by building index and soil index [37], [38], and the temperature index [39], [40]. On this basis, PCA [33] was used to determine the weight of each index and evaluate the regional EE. The specific calculation formula of the model is shown in Table I.

C. Remote Sensing Ecological Index Considering Full Elements (RSEIFE)

The RSEIFE model combines entropy weight method and moving window to replace the original PCA model to simulate the real ground EE formed by various elements (including water) in local areas and their interactions [29]. The entropy weight method can determine the objective weight according to the variability of the index. The greater the degree of dispersion of the index, the greater the weight of the index in the comprehensive index evaluation [41], [42], [43]. A moving window is constructed with each image pixel (*i, j*) as the center and 133 pixels as the window length [21], thus taking into account the ecological significance of features at the regional scale. The model calculation formula is as follows:

$$E_j = -\ln(n)^{-1} \sum_{i=1}^{n} p_{ij} \ln(p_{ij}) \tag{2}$$

where E_j is the information entropy of the index, n is the number of different values in each index, and p_{ij} is the probability that the ith value appears in the jth index. The weight value of the *j*th index can be expressed as follows:

$$W_j = \frac{1 - E_j}{m - \sum Ej} (j = 1, 2 \ldots m) \tag{3}$$

where W_j is the weight of each index and *m* is the number of EE evaluation indexes

$$\begin{aligned} \text{RSEIFE} = {} & W_{1(i,j)} * \text{NDVI} + W_{2(i,j)} * \text{WET} \\ & + W_{3(i,j)} * \text{NDBSI} + W_{4(i,j)} * \text{LST} \end{aligned} \tag{4}$$

TABLE I
FORMULAE FOR CALCULATING RSEI

Ecological indexes	Calculation formula	Explanation
Greenness	$\mathrm{NDVI} = \frac{\rho_{\mathrm{NIR}} - \rho_{\mathrm{Red}}}{\rho_{\mathrm{NIR}} + \rho_{\mathrm{Red}}}$	ρ_{Red}, ρ_{Green}, ρ_{Blue}, ρ_{NIR}, ρ_{SWIR1}, ρ_{SWIR2} represent the reflectance of red, green, blue, near infrared, short wave infrared 1 and short-wave infrared 2, respectively. T is the brightness temperature; RESI_0 is the initial ecological index value of the study area. f refers to the use of principal component analysis to determine the weight of each index and to solve its RSEI value.
Wetness	$\mathrm{WET} = \delta_1\rho_{\mathrm{Blue}} + \delta_2\rho_{\mathrm{Green}} + \delta_3\rho_{\mathrm{Red}} + \delta_4\rho_{\mathrm{NIR}} + \delta_5\rho_{\mathrm{SWIR1}} + \delta_6\rho_{\mathrm{SWIR2}}$	
Dryness	$\mathrm{NDSI} = (\mathrm{SI} + \mathrm{IBI})/2$ $\mathrm{SI} = \frac{(\rho_{\mathrm{SWIR1}} + \rho_{\mathrm{Red}}) - (\rho_{\mathrm{NIR}} + \rho_{\mathrm{Blue}})}{(\rho_{\mathrm{SWIR1}} + \rho_{\mathrm{Red}}) + (\rho_{\mathrm{NIR}} + \rho_{\mathrm{Blue}})}$ $\mathrm{IBI} = \frac{2\times\rho_{\mathrm{SWIR1}}/(\rho_{\mathrm{SWIR1}} + \rho_{\mathrm{NIR}}) - [\rho_{\mathrm{NIR}}/(\rho_{\mathrm{NIR}} + \rho_{\mathrm{Red}}) + \rho_{\mathrm{Green}}/(\rho_{\mathrm{Green}} + \rho_{\mathrm{SWIR1}})]}{2\times\rho_{\mathrm{SWIR1}}/(\rho_{\mathrm{SWIR1}} + \rho_{\mathrm{NIR}}) + [\rho_{\mathrm{NIR}}/(\rho_{\mathrm{NIR}} + \rho_{\mathrm{Red}}) + \rho_{\mathrm{Green}}/(\rho_{\mathrm{Green}} + \rho_{\mathrm{SWIR1}})]}$	
Heat	$\mathrm{LST} = T/[1 + (\lambda T/\rho)\times\ln\varepsilon] - 273.15$	
RSEI	$\mathrm{RSE}I = f(\mathrm{Greeness}, \mathrm{Wetness}, \mathrm{Dryness}, \mathrm{Heat})$ $\mathrm{RSE}I_0 = 1 - \mathrm{PC1}(\mathrm{NDVI}, \mathrm{WET}, \mathrm{LST}, \mathrm{NDBSI})$	

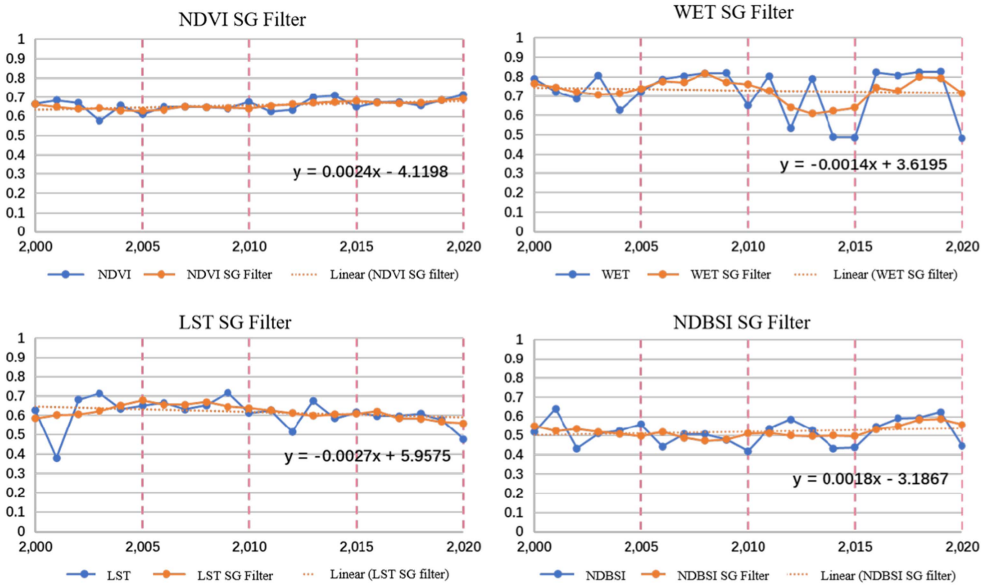

Fig. 2. Mean value curve of each ecological indexes before and after SG filter from 2000 to 2020.

where $W_{1(i,j)}$, $W_{2(i,j)}$, $W_{3(i,j)}$, and $W_{4(i,j)}$ are the weight values of the (i, j) image elements corresponding to NDVI, WET, NDBSI, and LST, respectively.

IV. RESULTS

A. Reconstruction of Ecological Index Time-Series Curve

Ecological index represents the changes of regional EE from various aspects. We calculated the average values of four ecological indexes for WUDZ and normalized these ecological indexes for the years 2000, 2005, 2010, 2015, and 2020. The time series of ecological indexes are constructed based on unified dimension, and the time series of four indexes is reconstructed by SG filter. Before the filtering reconstruction, the mean value of ecological indexes fluctuates greatly, and individual values far deviate from the fitting line, especially the WET index, which changes very irregularly in some years, and the fluctuation changes violently. In order to eliminate the effect of noise, SG filtering was used to reconstruct the time series. It can be seen in Fig. 2 that the time-series curve after SG filtering not only removes irregular fluctuations, but also retains the linear trend of the original data.

B. Temporal Change Analysis of Mean Value of Ecological Indexes Based on RSEIFE

From the perspective of the overall trend of each ecological indexes from 2000 to 2020, NDVI and NDBSI exhibited a slight increasing trend, while WET and LST displayed a slight downward trend. This suggests an overall rise in greenness, temperature, and dryness in the WUDZ and a decrease in wetness over the two decades. Despite the filtering process, certain years still exhibit noticeable changes in the values of WET and LST. For a more in-depth analysis, we have opted to conduct EE assessment once every five years in subsequent studies—specifically, for the years 2000, 2005, 2010, 2015, and 2020. As depicted in Fig. 2, data points for the four ecological indexes at these five-time

TABLE II
DISTRIBUTION OF WEIGHT VALUES OF EACH ECOLOGICAL INDEXES

	NDVI			WET			NDBSI			LST		
	Min	Max	**Mean**	Min	Max	**Mean**	Min	Max	**Mean**	Min	Max	**Mean**
2000	0.12	0.90	**0.40**	0.01	0.13	**0.06**	0.05	0.61	***0.38***	0.01	0.47	**0.16**
2005	0.07	0.81	***0.29***	0.02	0.25	**0.10**	0.11	0.74	**0.46**	0.02	0.54	**0.14**
2010	0.04	0.82	**0.32**	0.02	0.40	**0.16**	0.05	0.43	**0.24**	0.02	0.84	***0.28***
2015	0.19	0.99	**0.61**	0.00	0.15	**0.04**	0.01	0.36	**0.13**	0.00	0.74	***0.22***
2020	0.17	0.95	**0.44**	0.00	0.17	**0.05**	0.03	0.61	***0.36***	0.01	0.43	**0.15**

Note: The bolded values in the table are the mean values of the factors, and the underlined values are the values with the highest contribution to RSEIFE during the year.

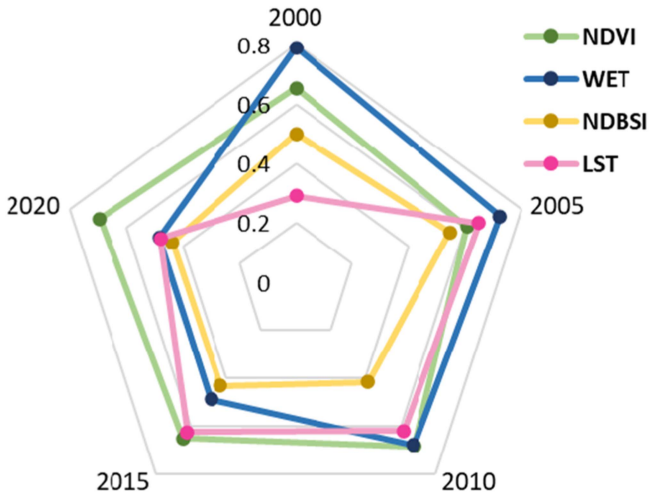

Fig. 3. Mean value of ecological indexes in 2000, 2005, 2010, 2015, 2020.

nodes closely align with the fitting line, indicating more stable values that better represent changes in ecological indexes during these intervals. The distribution of the mean values of ecological indexes in the past five years is shown in Fig. 3. NDVI experienced relatively minor changes, displaying a slight decrease followed by an increase. LST exhibited a lower value in 2000, increased more in 2005, fluctuated less from 2005 to 2015, and then decreased in 2020. WET changed greatly, mainly showing a decreasing trend compared to 2000. With a more pronounced decline in 2020. NDBSI demonstrated a pattern of increasing and then decreasing every five years, reaching its highest value in 2005 and display less fluctuation from 2010 to 2020. The most drastically changing ecological indexes are WET and LST, indicating that wetness and heat underwent more pronounced shifts from 2000 to 2020.

C. Changes of Ecological Indexes Weights Based on RSEIFE

The weights of the four ecological indexes for WUDZ were calculated using RSEIFE for the years 2000, 2005, 2010, 2015, and 2020, respectively (see Table II). The RSEIFE model employed a moving window to divide the study area into multiple zones, conducting individual calculations for each windowed zone. Consequently, the weights obtained for each ecological index exhibit spatial continuity and numerical intervals. A larger interval value indicates a more unbalanced distribution of an ecological index in the region.

RSEIFE utilizes the entropy method for weight allocation, whereby smaller fluctuation in ecological index value across the whole study area correspond to smaller weight value, and vice versa. It can be seen from Table II, for the ecological index that mainly affects the EE, NDVI consistently demonstrated the highest mean weight value in 2000, 2010, 2015, and 2020, with mean values of 0.40, 0.32, 0.61, and 0.44. respectively. This suggests that greenness is the main ecological index affecting the EE of this region in those years. In 2000 and 2020, The mean NDBSI exhibited the second highest mean weight values, registering values of 0.38 and 0.36, respectively, indicating a significant role of dryness in the EE in those years. In 2010 and 2015, the weighted mean value of LST ranked second-highest, highlighting substantial role of heat in the EE in those years. In 2005, NDBSI had the highest weighted value at 0.46, followed by NDVI, indicating that dryness was the main ecological index affecting the EE in that year, followed by greenness. From Table II, it can be seen that WET consistently exhibited lower weight values, indicating a more even distribution of wetness in the study area. Compared to the other three ecological indexes, wetness had a weaker impact on the EE of the study area.

D. Ecological Environment Grades Changes Based on RSEIFE

The obtained ecological index weight maps were multiplied and summed with the ecological index maps using ArcGIS to calculate the RSEIFE for the years 2000, 2005, 2010, 2015, and 2020, respectively. The RSEIFE values were then divided into five grades using the equal interval method, corresponding to the five ecological environment grades (EEGs). They are: poor (0–0.2), fair (0.2–0.4), moderate (0.4–0.6), good (0.6–0.8), and excellent (0.8–1.0) [33] (see Fig. 4). The calculated five-year mean RSEIFE values were 0.53, 0.57, 0.55, 0.64, and 0.47, respectively, with the EEGs for 2000, 2005, 2010, and 2020 all being moderate, while the EEGs for 2015 was good. The overall trend showed an initial increase followed by a decrease. Although the EEG values remained relatively stable from 2000 to 2020, the spatial distribution of the EE underwent significant changes. In 2000, areas with poor EEGs were concentrated in the main urban area of Wuhan. By 2010, regions with excellent EEGs had shifted to the east. With the development of the urban development area concept, areas with poor EEGs and fair EEGs spread out from the main urban area. In 2012, Wuhan City promulgated the "Wuhan Urban Development Area 1:2000 Basic Ecological Control Line Fall Line Plan," which clarified the development pattern of urban areas, and emphasized EE protection. Consequently, the quality of the EE generally improved by 2015. However, in 2020, the overall EEGs declined. the extent of urbanization reached its highest grade, and the

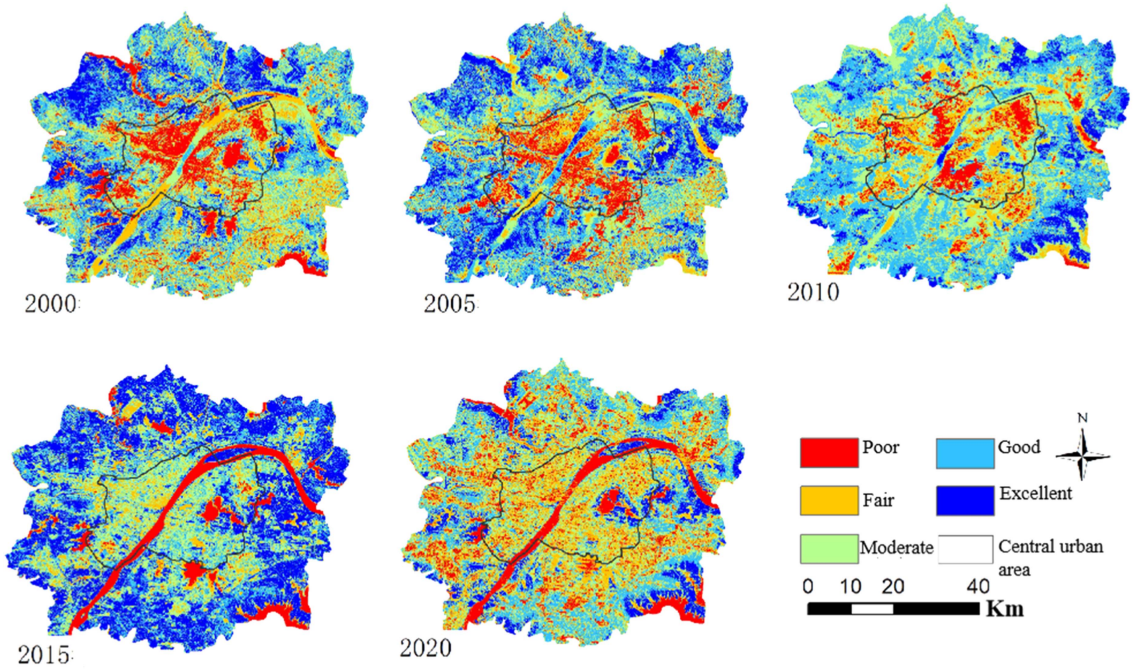

Fig. 4. Classification of RSEIFE from 2000 to 2020.

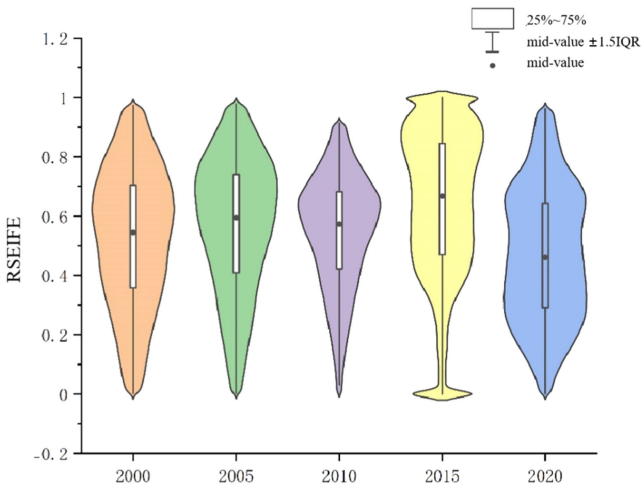

Fig. 5. RSEIFE density distribution map.

EEGs was predominantly poor. Areas with good EEGs and excellent EEGs were mainly distributed near the ring line of the urban development area and around the water area, resulting in relatively narrow ecological spaces.

Statistics of RSEIFE on years 2000, 2005, 2010, 2015, and 2020 were analysis to produce a violin plot (see Fig. 5) that shows the distribution of RSEIFE values and their probability densities over these five years. In 2000, the RSEIFE values are more concentrated near the mean, with the main distribution range between 0.4 and 0.8, indicating moderate to good grades. The overall distribution is more uniform and smoother. By 2005, the RSEIFE values are primarily concentrated in the 0.6–0.8 range. Compared to 2000, the distribution shape is similar, but the overall data distribution has shifted upwards. In 2010, the data density distribution becomes more concentrated, the RSEIFE slightly decreases, and a more prominent peak appears near 0.6. By 2015, the RSEIFE distribution is mainly in the range of 0.4–1. The shape is wider and longer, the distribution is gentler, lacks a clear peak, and has more outliers, indicating a downward trend. This year also shows greater data discrepancy. In 2020, the distribution is wide and gentle, with two peaks vaguely on both sides of the median value, and the overall ecological value is lower. From the quartiles and the overall shape of the distribution, the RSEIFE distributions of 2000, 2005, and 2010 are relatively similar, while those of 2015 and 2020 are more distinct.

E. Monitoring of EEGs Change

In order to better explore the spatial differences in EEGs change in this study area during these 20 years. The change information of RSEIFE from 2000 to 2020 was counted based on the reclassification results of ArcGIS, and the map of EEGs change was generated (see Fig. 6), as well as the area of EEGs change and the percentage of the area occupied by them were counted. A total of nine types of class changes were calculated, namely –4, –3, –2, –1, 0, 1, 2, 3, and 4, with a negative number indicating a decrease in EEGs compared to the previous year, that means ecological environment deterioration (EED). 0 indicating no change in EEGs in these two years (EEU), and a positive number indicating an increase in EEGs, that is ecological environment improvement (EEI).

It can be seen from Table III that the changes of EEG in 2005 compared with that in 2000 were mainly concentrated in grades 1–2 and the region with change grade 0 accounted for the highest proportion, accounting for 38.52% of the whole study area, mainly distributed in the relatively stable central urban area. The area of EEGs improvement accounted for 37.65%, and the main distribution area was around large rivers and Qingshan District. The proportion of EED to grade –1 was 17.26%, which

TABLE III
AREA AND PERCENTAGE OF CHANGE IN ECOLOGICAL ENVIRONMENT CLASSES IN WUDZ

		EEI			EEU			EED		
Difference in grade change		4	3	2	1	0	-1	-2	-3	-4
2000–2005	Area (Km^2)	13.81	64.44	316.68	1032.96	1460.89	654.47	187.4	52.27	9.32
	Percentage of change	0.36%	1.70%	8.35%	27.24%	38.52%	17.26%	4.94%	1.38%	0.25%
	Total		37.65%			38.52%		23.82%		
2005–2010	Area (Km^2)	1.78	26.79	199.24	790.54	1495.77	970.16	261.88	41.43	4.65
	Percentage of change	0.05%	0.71%	5.25%	20.85%	39.44%	25.58%	6.91%	1.09%	0.12%
	Total		26.85%			39.44%		33.70%		
2010–2015	Area (Km^2)	3.94	60.72	558.66	1437.69	978.93	443.06	246.72	59.81	7.21
	Percentage of change	0.10%	1.60%	14.71%	37.87%	25.78%	11.67%	6.50%	1.58%	0.19%
	Total		54.28%			25.78%		19.93%		
2015–2020	Area (Km^2)	0.57	5.6	30.43	216.95	1257.11	1538.63	540.81	160.75	45.88
	Percentage of change	0.01%	0.15%	0.80%	5.71%	33.11%	40.53%	14.24%	4.23%	1.21%
	Total		6.68%			33.11%		60.21%		

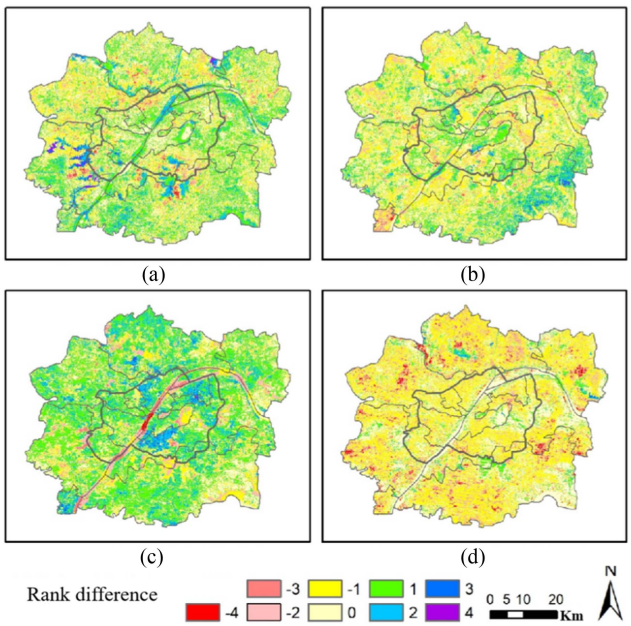

Fig. 6. Map of changes in EEGs. (a) EEGs changes from 2000 to 2005. (b) EEGs changes from 2005 to 2010. (c) EEGs changes from 2010 to 2015. (d) EEGs changes from 2015 to 2020.

was mainly distributed in Dongxihu District, Huangpi District, and Xinzhou District, because the number of scattered lakes and pits was significantly reduced, and at the same time, these three districts gradually began urbanization construction activities. Compared with 2005, the change of EEGs in 2010 was mainly concentrated in the range of –2–1 grade, with a total proportion of 92.78%, and the area of EED increased, accounting for 33.70%, most of which were distributed in WUDZ outside the main urban area. The scope of urbanization construction was relatively extensive and the construction degree was relatively intense. The proportion of EEI is 26.85%, which is mainly distributed in the boundary of the four-ring road, especially around the water area. In 2020, compared with 2015, the changes of EEGs were mainly concentrated in –2–1 grades, with a total proportion of 93.59%, and the EEI area accounted for a relatively small proportion of 6.68%, which was mainly distributed in lake wetland area. The area of EED accounted for 60.21%, and the study area showed EED. It is worth mentioning that ecology has cumulative benefits and lag, and urbanization construction activities will slow down in 2020 compared with 2015, but the overall construction land area of WUDZ has reached the largest, the scale of urbanization has reached the peak, and the EE reflects a low state.

F. Temporal Changes of Ecological Environment in Typical Regional Urban Expansion

Currently, China is undergoing rapid urbanization, leading to the saturation of construction land within cities. To meet the growing demand for urban construction land, urban lakes are being filled and repurposed, resulting in a significant reduction in the size of lake areas. In this context, conflicts arise between urban lakes and development, creating a contradiction between the preservation of urban lakes and the expansion of construction land [44]. This study focuses on Shahu Lake, the sole lake within the inner ring road of WUDZ, as an illustrative case. Satellite images and EE comparison maps of Shahu Park from 2000 to 2020 are presented (see Fig. 7) to explore the changes in the EE during the interaction between lakes and urban construction.

Fig. 7 clearly depicts the destruction and encroachment on the lake during the period of urban construction from 2000 to 2020. In 2000, the urban construction filled a portion of the lake, and subsequent real estate development and road construction further encroached on the sand lake from the southeast, northwest, and north over the following decade. During this period, the EE around the sand Lake experienced fluctuations. The intensified development activities from 2000 to 2005 resulted in a poor EE around the Sand Lake. The EEGs of the transition boundary between the lake and the residential area is medium

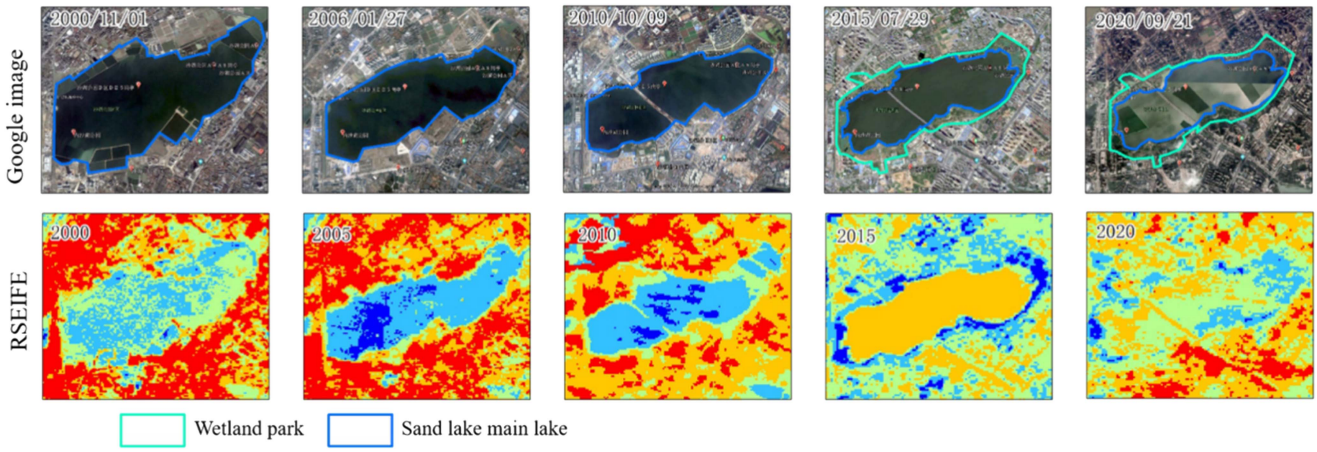

Fig. 7. Satellite images and ecological environment comparison maps of Shahu Park from 2000 to 2020.

and good. As the construction activities entered a stable period, the ecological benefits of the water body for the surrounding environment began to be manifest, resulting in an improvement in the EEGs around the sand lake in 2010.

In 2012, the construction of Sand Lake Park began, focusing on the development of lake wetlands and park green space. From 2015 to 2020, a symbiotic relationship between the lake and urban construction emerged, with minimal changes to the main lake boundary. During this period, the EE of the park wetland and green space excelled, positively impacting the surrounding environment. In 2020, extreme weather events, including heavy rainfall and flooding, lead to slight environment changes, but the overall distribution remained similar to that in 2015. In general, the changes of urban EE are driven by both natural resource shifts and human activities. The change of natural resources is affected by weather and precipitation, but human activities, particularly construction, play a more significant role. Therefore, when proposing policies and regulations for ecological protection and restoration in urban construction, it is advisable to adopt a comprehensive approach that considers both the protection of natural resources and the constraints on the scope of urban construction areas.

V. Discussion

A. Time-Series Analysis of Ecological Environment

From the overall trend of ecological indexes in WUDZ from 2000 to 2020, WET and LST showed a slight decrease. This suggests a decline in wetness and heat in WUDZ over these two decades, possibly attributable to shifts in the distribution of green vegetation and impervious surfaces. Notably, due to significant change in land use types away from the main urban area and the rapid development of urbanization, spatial disparities exist between EE of WUDA and that of the main urban area of Wuhan.

From the overall changes in the area and proportion of EE grade in WUDZ from 2000 to 2020, the areas with poor EEG in 2000 were concentrated in the main urban area, while the northern suburban waters were numerous and scattered, with good and excellent EEGs, and the southern waters were extensive and sparse, with medium and poor EEGs.

In 2005, the areas with poor EEGs gradually spread to the periphery of the main urban area, with Xinzhou District in the northeast and part of Jiangxia District in the south showing poor EEGs. In 2010, the area with excellent EEG was shifted to the east. With the proposal of the concept of WUDZ development and the intensification of urbanization, the overall EEQ declined. The area with poor and fair EEGs spread out from the main urban area, and the construction in the north also began to intensify.

In 2012, Wuhan City promulgated the "Wuhan Urban Development Area 1:2000 Basic Ecological Control Line Delimitation Plan," which clarified the development pattern of WUDZ, and paid attention to ecological protection while urbanization construction. In 2015, the EEQ was generally improved, the EEGs of the urban area were poor or medium, and the outer ring of WUDZ showing excellent EEGs. The EEG of the central water surface of large area water body is poor.

In 2020, the overall EEQ shows a decline, the boundary of urbanization construction reaches the highest grade, the urbanization development of all districts of the new city is more uniform, and the EEGs mainly shows poor or fair. The areas with excellent and good EEGs are mainly distributed near the WUDZ Ring line and around the water area, and the ecological space is relatively narrow. It is worth mentioning that extreme weather such as heavy rainfall and flooding occurred in the summer of 2020, and the EE changes caused by these events have not been specifically studied yet.

B. RSEIFE and Land Use

The distribution changes in the EE were further analyzed in conjunction with and use types. From 2000 to 2020, urban areas expanded significantly from main urban regions to urban development zones. The number of lake waters decreased during this period. Compared to year 2000, construction activities in 2005 were concentrated in the main urban area of Wuhan and gradually expanded to the outskirts, with more noticeable signs of engineering activities. In 2010, the Master Plan of Wuhan City (2010–2020) was introduced, focusing on increasing construction land primarily around the main urban area. By 2020, construction activities in Wuhan's central urban area had

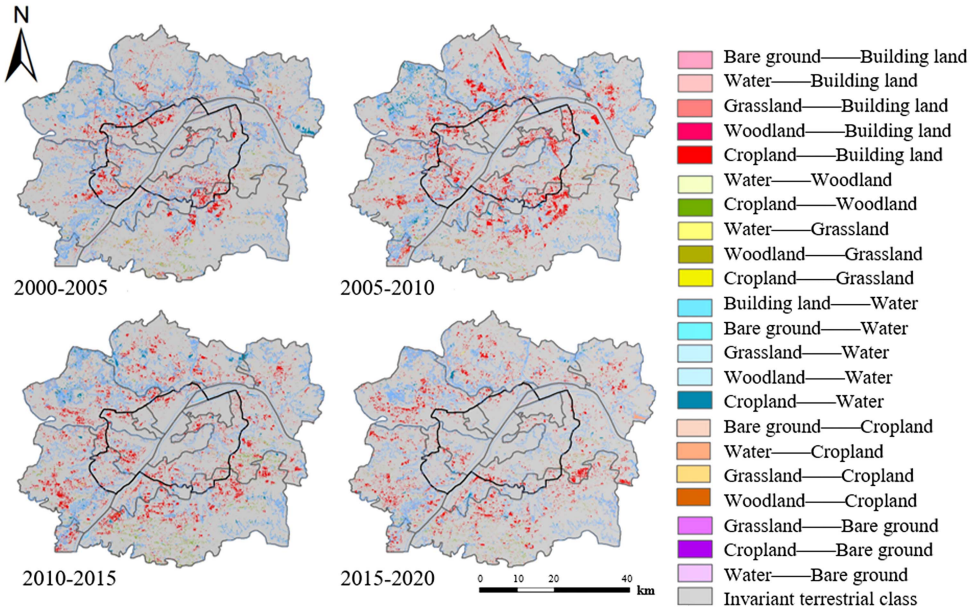

Fig. 8. Map of changes in land-use categories.

stabilized. The development orientation of the six new cities shows varying demands for land and different development degrees of development, leading to differences in in spatial distribution of EEQ.

Fig. 8 illustrates the changes in lakes, rivers and other water areas. Based on the water area extents in 2000, many lakes have disappeared or shrunk. Notably, lake protection efforts have been gradually implemented since 2007, with the “Three Lines and One Road” Protection Plan for Lakes in Central Urban Areas of Wuhan City" being promulgated in 2014. This plan significantly extended the scope of lake protection. Following its implementation, lake areas have increased. From 2005 to 2020, some cultivated lands reverted to lakes, shifting ecological development from “lake to field” to “field to lake,” which negatively impacted the surrounding environment.

Based on the developmental-ecological spatial pattern, it is evident that the spatial distribution of the EE is strongly correlated with land use changes and policy drivers. The EEGs for construction land are poor, while those for cultivated land and forest land are good to medium. The EEGs of shallow waters and wetlands around water areas are generally excellent or good. With the expansion of urban areas, regions with poor EEGs are also expanding, reflecting the self-regulation and development ability of human beings concerning urban ecosystems. To create ecological cities, it is essential to apply ecological principles and modern scientific and technological means to harmonize the relationship between urban, social, economic, engineering and other artificial ecosystems with natural ecosystems.

C. Limitations and Future Work

In this study, RSEIFE model was used to solve the problems of inability to consider the overall ecological environmental benefits of water elements, and to provide a more realistic ecological simulation effect based on the ecological impact range window. However, there are still several aspects to be improved in the process of constructing the model. There is a lack of more exploration on the processing methods of long time-series data.

1) There are many studies on data screening and fusion methods based on GEE, and in this article, we select the median synthesis, SG filtering, and time-series interpolation commonly used in time-series research for remote sensing data generation, and we do not take more comparative data processing methods, and the issue of the quality of the data products needs to be further researched.
2) The years of the research are selected at a long interval. Due to the limitation of time and computational efficiency, five years were chosen as the interval for one study, which ignored the ecological details of changes in many years, and a one-year interval can be considered to further determine the driving factors of ecological changes.
3) The application of the RSEIFE lacks the analysis of changes in ecological results for the water body itself. Since the water environment is a large research direction, this article is more about the water body as a whole to study the ecological benefits of the water body to the surrounding environment as well as the study area, and lacks the research interpretation of the EE of the water body itself.

In the future research, we should pay attention to the advantages of GEE in the application of large-scale EE evaluation, and realize the continuous monitoring of large-scale and long-time sequence of EE. At the same time, in the application of the analysis process for the water body as a specific feature, it is necessary to combine more aspects such as water eutrophication, water quality changes and other perspectives to interpret the changes in the water EE. In addition, the selection of ecological

indexes can be more diversified according to the characteristics of the study area and the different purposes of the study, for example, the convening of the Conference on Biological Diversity, which provides new ideas for the EE evaluation system, the Ministry of Ecology and Environment has proposed that biodiversity indexes be included in the framework of the EE evaluation. In the future, the whole EE evaluation and analysis system will be further improved to expand the depth and breadth of its research, and to provide more detailed and accurate EE inversion and geographic interpretation of the surface.

VI. Conclusion

In this study, RSEIFE was used to analyze the spatial distribution of WUDZ EE from 2000 to 2020, considering the characteristics of spatial total indexes and local detection. Combined with the change of land use type, the article further describes the process of urban expansion and the change of lake water area. At the same time, it analyzes the driving factors of EE change in WUDZ with the example of urbanization construction and ecological space change. The results show that from 2000 to 2020, the EEQ of WUDZ presents a trend of first increasing and then decreasing, and the fluctuation is small. At the same time, the changes of EE show that the EEG of the main urban area of WUDZ is worse. With the urbanization process moving toward the "six new cities" and approaching the Fourth Ring Road, the EEG of the outer suburbs is gradually deteriorating. The EEG of urban agglomeration area is poor, and the EEG around the lake are generally high, which indicates that the construction land has negative benefits on the surrounding environment while the lake resources have positive benefits on the ecology of the study area. Combining land use type and RSEIFE results, it is found that EEG is related to land use. The results of RSEIFE and the process of urban development reveal that the driving factors of EE change in WUDZ from 2000 to 2020 are the intensification of urbanization and the reduction of lake resources, and the urbanization process and lake resources encroachment show a causal relationship. The establishment of lake wetland park and green park leads to the increase of greenness and wetness, which is reflected in the improvement of the surrounding EE. Lake resources have important positive benefits for the overall EE of the city. Both the urbanization process and lake resource protection are driven by policies. Rational formulation of policies and planning to develop ecological space and limit urban construction space is the key to ensure the sustainable development of urban EE.

References

[1] T. Chen, Z. Lu, Y. Yang, Y. Zhang, B. Du, and A. Plaza, "A Siamese network based U-Net for change detection in high resolution remote sensing images," *IEEE J. Sel. Top. Appl. Earth Observ. Remote Sens.*, vol. 15, pp. 2357–2369, Apr. 2022.

[2] X. Chen et al., "A spatiotemporal interpolation graph convolutional network for estimating $PM_{2.5}$ concentrations based on urban functional zones," *IEEE Trans. Geosci. Remote Sens.*, vol. 61, Dec. 2022, Art. no. 4100114.

[3] T. Zhang, Y. Sun, X. Zhang, L. Yin, and B. Zhang, "Potential heterogeneity of urban ecological resilience and urbanization in multiple urban agglomerations from a landscape perspective," *J. Environ. Manage.*, vol. 342, May 2023, Art. no. 118129.

[4] X. Ma et al., "XGBoost-based analysis of the relationship between urban 2D/3D morphology and seasonal gradient land surface temperature," *IEEE J. Sel. Top. Appl. Earth Observ. Remote Sens.*, vol. 17, pp. 4109–4124, Jan. 2024.

[5] S. Tian et al., "A cross-scale study on the relationship between urban expansion and ecosystem services in China," *J. Environ. Manage.*, vol. 319, Aug. 2022, Art. no. 115774.

[6] Q. Lan, J. Dong, S. Lai, N. Wang, L. Zhang, and M. Liao, "Flood inundation extraction and its impact on ground subsidence using sentinel-1 data: A case study of the '7.20' rainstorm event in Henan Province, China," *IEEE J. Sel. Topics Appl. Earth Observ. Remote Sens.*, vol. 17, pp. 2927–2938, Jan. 2024.

[7] Y. Song, "Ecological city and urban sustainable development," *Procedia Eng.*, vol. 21, pp. 142–146, Jan. 2011.

[8] S. Jalayer, A. Sharifi, D. Abbasi-Moghadam, A. Tariq, and S. Qin, "Assessment of spatiotemporal characteristic of droughts using in situ and remote sensing-based drought indices," *IEEE J. Sel. Topics Appl. Earth Observ. Remote Sens.*, vol. 16, pp. 1483–1502, Jan. 2023.

[9] T. Chen, Q. Wang, Z. Zhao, G. Liu, J. Dou, and A. Plaza, "LCFSTE: Landslide conditioning factors and swin transformer ensemble for landslide susceptibility assessment," *IEEE J. Sel. Topics Appl. Earth Observ. Remote Sens.*, vol. 17, pp. 6444–6454, Mar. 2024.

[10] T. Chen et al., "BisDeNet: A new lightweight deep learning-based framework for efficient landslide detection," *IEEE J. Sel. Topics Appl. Earth Observ. Remote Sens.*, vol. 17, pp. 3648–3663, Jan. 2024.

[11] C. Wang, T. Chen, and A. Plaza, "MFE-ResNet: A new extraction framework for land cover characterization in mining areas," *Future Gener. Comput. Syst.*, vol. 145, pp. 550–562, 2023.

[12] C. Liu, J. Liu, Q. Zhang, H. Ci, X. Gu, and A. Gulakhmadov, "Attribution of NDVI dynamics over the globe from 1982 to 2015," *Remote Sens.*, vol. 14, no. 11, Jun. 2022, Art. no. 2706.

[13] N. T. Son, C. F. Chen, C. R. Chen, V. Q. Minh, and N. H. Trung, "A comparative analysis of multitemporal MODIS EVI and NDVI data for large-scale rice yield estimation," *Agric. Forest Meteorol.*, vol. 197, pp. 52–64, Jun. 2014.

[14] M. K. Firozjaei, S. Fathololoumi, M. Kiavarz, A. Biswas, M. Homaee, and S. K. Alavipanah, "Land surface ecological status composition index (LSESCI): A novel remote sensing-based technique for modeling land surface ecological status," *Ecol. Indicators*, vol. 123, Jan. 2021, Art. no. 107375.

[15] L. C. Messer, J. S. Jagai, K. M. Rappazzo, and D. T. Lobdell, "Construction of an environmental quality index for public health research," *Environ. Health*, vol. 13, no. 1, pp. 1–22, May 2014.

[16] X. Liao, W. Li, and J. Hou, "Application of GIS based ecological vulnerability evaluation in environmental impact assessment of master plan of coal mining area," *Procedia Environ. Sci.*, vol. 18, pp. 271–276, Jan. 2013.

[17] J. Zhang, H. Li, D. Huang, and X. Wang, "Evaluation study of ecological resilience in southern red soil mining areas considering rare earth mining process," *Sustainability*, vol. 15, no. 3, Feb. 2023, Art. no. 2258.

[18] H. Xu, Y. Wang, H. Guan, T. Shi, and X. Hu, "Detecting ecological changes with a remote sensing based ecological index (RSEI) produced time series and change vector analysis," *Remote Sens.*, vol. 11, no. 20, Oct. 2019, Art. no. 2345.

[19] J. Pan, H. Li, and Y. Li, "Spatiotemporal change analysis of environmental quality in mining areas based on long-term landsat images," *Geocarto. Int.*, vol. 37, no. 26, pp. 11052–11067, Mar. 2022.

[20] D. Zhu, T. Chen, Z. Wang, and R. Niu, "Detecting ecological spatial-temporal changes by remote sensing ecological index with local adaptability," *J. Environ. Manage.*, vol. 299, Sep. 2021, Art. no. 113655.

[21] C. Li, T. Chen, K. Jia, and A. Plaza, "Coupling analysis between ecological environment change and urbanization process in the middle reaches of Yangtze River Urban Agglomeration, China," *IEEE J. Sel. Topics Appl. Earth Observ. Remote Sens.*, vol. 15, pp. 2357–2369, Jun. 2024.

[22] J. Wang, J. Ma, F. Xie, and X. Xu, "Improvement of remote sensing ecological index in arid regions: Taking Ulan Buh Desert as an example," *Chin. J. Appl. Ecol.*, vol. 31, no. 11, pp. 3795–3804, Nov. 2020.

[23] D. Zhu, T. Chen, R. Niu, and N. Zhen, "Analyzing the ecological environment of mining area by using moving window remote sensing ecological index," *Geomatics Inf. Sci. Wuhan Univ.*, vol. 46, no. 3, pp. 341–347, Jan. 2021.

[24] W. Liao and W. Jiang, "Evaluation of the spatiotemporal variations in the eco-environmental quality in China based on the remote sensing ecological index," *Remote Sens.*, vol. 12, no. 15, Aug. 2020, Art. no. 2462.

[25] Z. Wu, M. Wu, S. Cai, and D. Zhu, "Monitoring and evaluation of ecological environment's spatio-temporal variation in mine based on RSEI in Yongding mine," *Ecologic Sci.*, vol. 35, no. 5, pp. 200–207, Oct. 2016.

[26] C. J. Sun, W. Q. Zhang, X. G. Li, and J. L. Sun, "Evaluation of ecological effect of gully region of loess plateau based on remote sensing image," *Trans. CSAE*, vol. 35, no. 12, pp. 165–172, Jun. 2019.
[27] L. Cheng, Z. Wang, S. Tian, Y. Liu, M. Sun, and Y. Yang, "Evaluation of eco-environmental quality in Mentougou District of Beijing based on improved remote sensing ecological index," *Chin. J. Ecol.*, vol. 40, no. 4, Feb. 2021, Art. no. 1177.
[28] J. Li, J. Liang, Y. Wu, S. Yin, Z. Yang, and Z. Hu, "Quantitative evaluation of ecological cumulative effect in mining area using a pixel-based time series model of ecosystem service value," *Ecol. Indic.*, vol. 120, Jan. 2021, Art. no. 106873.
[29] Z. Wang, T. Chen, D. Zhu, K. Jia, and A. Plaza, "RSEIFE: A new remote sensing ecological index for simulating the land surface eco-environment," *J. Environ. Manage.*, vol. 326, Nov. 2023, Art. no. 116851.
[30] A. Savitzky and M. J. Golay, "Smoothing and differentiation of data by simplified least squares procedures," *Anal. Chem.*, vol. 36, no. 8, pp. 1627–1639, Jul. 1964.
[31] J. Yang and X. Huang, "The 30 m annual land cover and its dynamics in China from 1990 to 2019," *Earth Syst. Sci. Data*, vol. 13, pp. 3907–3925, Aug. 2021.
[32] P. Kempeneers, M. Claverie, and R. D. Andrimont, "Using a vegetation index as a proxy for reliability in surface reflectance time series reconstruction (RTSR)," *Remote Sens.*, vol. 15, no. 9, Apr. 2023, Art. no. 2303.
[33] H. Xu, "A remote sensing index for assessment of regional ecological changes," *China Environ. Sci.*, vol. 33, no. 5, pp. 889–897, May 2013.
[34] S. N. Goward, Y. Xue, and K. P. Czajkowski, "Evaluating land surface moisture conditions from the remotely sensed temperature/vegetation index measurements: An exploration with the simplified simple biosphere model," *Remote Sens. Environ.*, vol. 79, nos. 2/3, pp. 225–242, Feb. 2002.
[35] E. P. Crist, "A TM tasseled cap equivalent transformation for reflectance factor data," *Remote Sens. Environ.*, vol. 17, no. 3, pp. 301–306, Jan. 1985.
[36] C. Chen, J. Fu, S. Zhang, and X. Zhao, "Coastline information extraction based on the tasseled cap transformation of Landsat-8 OLI images," *Estuarine, Coastal Shelf Sci.*, vol. 217, pp. 281–291, Feb. 2019.
[37] H. Xu, "A new index for delineating built-up land features in satellite imagery," *Int. J. Remote Sens.*, vol. 29, no. 14, pp. 4269–4276, Jan. 2008.
[38] F. Xu, H. Li, and Y. Li, "Ecological environment quality evaluation and evolution analysis of a rare earth mining area under different disturbance conditions," *Environ. Geochem. Health*, vol. 43, pp. 2243–2256, Nov. 2021.
[39] J. Zhang et al., "Evaluating water resource assets based on fuzzy comprehensive evaluation model: A case study of Wuhan city, China," *Sustainability*, vol. 11, no. 17, Sep. 2019, Art. no. 4627.
[40] Y. Cui, P. Feng, J. Jin, and L. Liu, "Water resources carrying capacity evaluation and diagnosis based on set pair analysis and improved the entropy weight method," *Entropy*, vol. 20, no. 5, May 2018, Art. no. 359.
[41] W. Xu, H. Liu, Q. Zhang, and P. Liu, "Response of vegetation ecosystem to climate change based on remote sensing and information entropy: A case study in the arid inland river basin of China," *Environ. Earth Sci.*, vol. 80, pp. 1–14, Feb. 2021.
[42] S. Das and D. P. Angadi, "Assessment of urban sprawl using landscape metrics and Shannon's entropy model approach in town level of Barrackpore sub-divisional region, India," *Model. Earth Syst. Environ.*, vol. 7, pp. 1071–1095, Oct. 2021.
[43] J. Ma, S. Huang, and Z. Xu, "Satellite remote sensing of lake area in Wuhan from 1973 to 2015," *Shuili Xuebao*, vol. 48, pp. 903–913, Aug. 2017.
[44] J. Wu, S. Yang, and X. Zhang, "Interaction analysis of urban blue-green space and built-up area based on coupling model—A case study of Wuhan Central City," *Water*, vol. 12, no. 8, Aug. 2020, Art. no. 2185.

Jiao Pan received the master's degree in geography from Jiangxi University of Science and Technology, Ganzhou, China, in 2023. She is currently working toward the Ph.D. degree in earth exploration and information technology with the China University of Geosciences, Wuhan, China.

Her current research interests include ecological environment monitoring and evaluation by remote sensing.

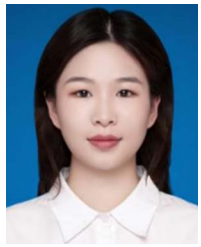

Ziwei Wang received the master's degree in resources and environment from the China University of Geosciences, Wuhan, China, in 2023.

She is currently an employee working with the 7th Geological Brigade, Hubei Geological Bureau, Yichang, China. Her research interests include ecological environment monitoring and evaluation by remote sensing.

Tao Chen (Senior Member, IEEE) received the Ph.D. degree in photogrammetry and remote sensing from Wuhan University, Wuhan China, in 2008.

He is currently an Associate Professor with the School of Geophysics and Geomatics, China University of Geosciences, Wuhan, China. He has authored or coauthored more than 60 scientific papers including IEEE TRANSACTIONS ON GEOSCIENCE AND REMOTE SENSING, IEEE JOURNAL OF SELECTED TOPICS IN APPLIED EARTH OBSERVATIONS AND REMOTE SENSING, *International Journal of Applied Earth Observation and Geoinformation*, etc., and guest edited ten journal special issues. From 2015 to 2016, he was a Visiting Scholar with the University of New South Wales, Sydney, Australia. His research interests include image processing, machine learning, and geological remote sensing.

Dr. Chen serves as the Associate Editor for IEEE JOURNAL OF SELECTED TOPICS IN APPLIED EARTH OBSERVATIONS AND REMOTE SENSING.

Kun Jia received the B.S. degree in surveying and mapping engineering from Central South University, Changsha, China, in 2006, the Ph.D. degree in cartography and GIS from the Institute of Remote Sensing Applications, Chinese Academy of Sciences, Beijing, China, in 2011.

He is currently a Professor with the State Key Laboratory of Remote Sensing Science and also with the Beijing Engineering Research Center for Global Land Remote Sensing Products, Faculty of Geographical Science, Beijing Normal University, Beijing. His main research interests include estimation of vegetation parameters, land cover classification, and agriculture monitoring using remote sensing data.

Antonio Plaza (Fellow, IEEE) received the M.Sc. and Ph.D. degrees in computer engineering from the Department of Technology of Computers and Communications, University of Extremadura, Badajoz, Spain, in 1999 and 2002, respectively.

He is currently a Full Professor and the Head of the Hyperspectral Computing Laboratory, Department of Technology of Computers and Communications, University of Extremadura. He has authored more than 600 publications and guest edited ten journal special issues. He has reviewed more than 500 manuscripts for more than 50 different journals.

Dr. Plaza served as the Editor-in-Chief for IEEE TRANSACTIONS ON GEOSCIENCE AND REMOTE SENSING from 2013 to 2017. He is included the Highly Cited Researchers List (Clarivate Analytics) from 2018 to 2020.